Title

A Convenient and Versatile Method To Control the Electrode Microstructure toward High-Energy Lithium-Ion Batteries

Journal

Nano Letters, 16(7)

ISSN

1530-6984

Authors

Zhao, Hui

Yang, Qing

Yuca, Neslihan

et al.

Publication Date

2016-07-13

DOI

10.1021/acs.nanolett.6b02156

Peer reviewed

A convenient and versatile method to control the electrode microstructure toward high-energy lithium-ion batteries

Hui Zhao,[a] Qing Yang,[c] Neslihan Yuca,[b] Min Ling,[a] Kenneth Higa,[a] Vincent S. Battaglia,[a] Dilworth Y Parkinson,[c] Venkat Srinivasan,[a] and Gao Liu[a*]

[a]*Energy Technologies Area,* [c]*Advanced Light Source, Lawrence Berkeley National Laboratory, Berkeley, California, 94720, United States*

[b]*Istanbul Technical University, Energy Institute, Istanbul, 34469, Turkey*

[*] Tel.: +1-510-486-7207; fax: +1-510-486-7303; Email: gliu@lbl.gov (G. Liu)

Abstract: Control over porous electrode microstructure is critical for the continued improvement of lithium ion batteries. This paper describes a convenient and economical method for controlling electrode porosity, thereby enhancing material loading and stabilizing the cycling performance of lithium ion electrodes. Sacrificial NaCl is added to a Si-based electrode, which demonstrates an areal capacity of ~4 mAh/cm^2 at a C/10 rate (0.51 mA/cm^2) and an areal capacity of 3 mAh/cm^2 at a C/3 rate (1.7 mA/cm^2), one of the highest material loadings reported for a Si-based anode at such a high cycling rate. X-ray microtomography confirmed the improved porous architecture of the SiO electrode with NaCl. This versatile method was also successfully applied to nanoSi and lithium iron phosphate electrodes. The method developed here is expected to be compatible with the state-of-the-art lithium ion battery industrial fabrication processes, and therefore holds great promise as a practical technique for boosting the electrochemical performance of lithium ion batteries without changing material systems.

Keywords: porosity, high-capacity anode, conductive polymer binder, X-ray tomography, high loading, lithium-ion battery

Introduction

Optimization of porous electrode microstructure is fundamentally important for the continued improvement of high performance lithium-ion batteries (LIBs).[1] Electrode architecture strongly influences cell properties such as active material loading, cycling rate, cell life, and safety. In typical industrial LIB electrode fabrication, active material particles and carbon conductive additives are suspended in a viscous polymer binder/solvent solution, and the resulting slurry is then cast and dried. Calendering is then frequently employed to generate a dense electrode with higher energy density and better rate performance.[2] However, the microstructure of the LIB electrode is not well controlled by this manufacturing process, so an ideal lithium ion transport is not achieved.

Control over electrode microstructure is especially critical for high capacity LIB electrodes such as Si or Sn alloy anodes. Compared to conventional electrode materials such as graphite or cobalt oxide, which experience less than 10% volume changes during cell cycling, these new electrode materials undergo huge volumetric changes (300% for Si) during charge and discharge. The resulting dramatic structural changes in the microstructures of these high-capacity anodes, severely limit the practical application of the high capacity electrode materials. Thus, it is imperative to develop a convenient method to control LIB electrode microstructure.

Traditionally, the biggest hurdles for controlling electrode architectures have been the relatively complex synthesis processes involved and their associated costs.[3] This article describes our use of a sacrificial agent (sodium chloride) to realize better control of LIB electrode architecture. The introduction and removal of this sacrificial reagent is environmentally friendly and compatible with state-of-the-art electrode fabrication processes.

Results and Discussion

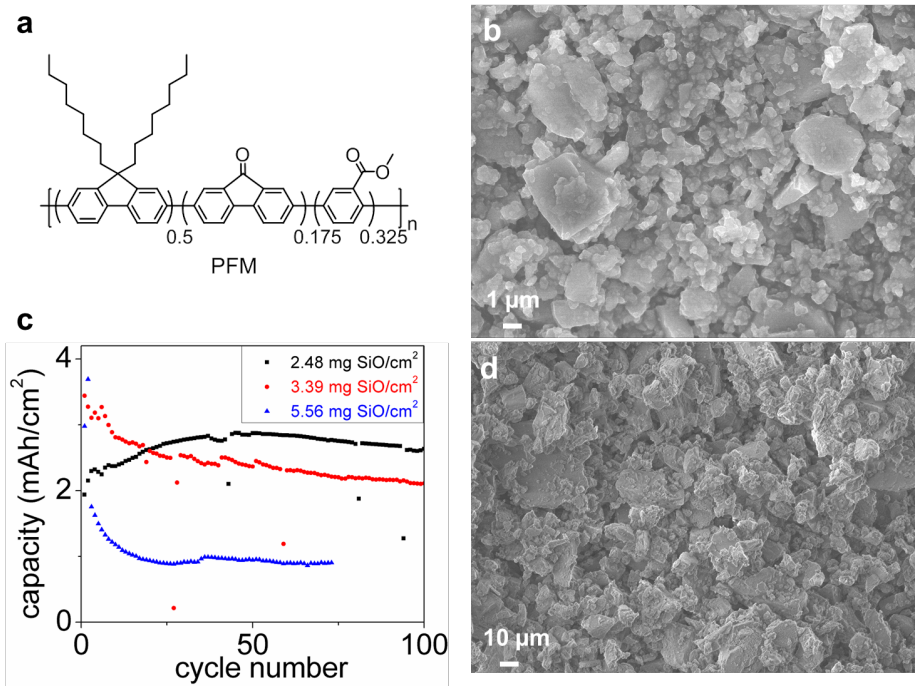

Figure 1. (a) Chemical structure of the PFM binder used in this work. (b) SEM image of SiO particles. (c) Areal capacity vs. cycle numbers with increasing SiO loading at C/10 (100 mA/g). (d) SEM image of ball-milled NaCl particles.

SiO electrodes were fabricated using a functional conductive polymer binder, poly (9,9-dioctylfluorene-co-fluorenone-co-methyl benzoic ester) (PFM, Figure 1a), which was previously developed by combining adhesive and electrically conductive domains to provide molecular-level electronic connections between the active material and the conductive polymer matrix.[4,5,6] We recently established the superior performance of the conductive functional PFM binder/SiO electrode, in which only 2% (by weight) binder is required to achieve stable cycling for ~500 cycles.[7] Since the polymer binder is in-situ doped and electronically conductive, carbon additives are not needed and thus the electrode used in this work is only composed of active material (90 wt% SiO) and polymer binder (10 wt% PFM). Figure 1b shows an SEM image of the pristine SiO active material particles. Particle size analysis via light scattering of these particles dispersed in water shows a bimodal particle size distribution, with peaks at particle diameters of

~1.5 µm and ~12 µm; this bimodal size distribution is evident in the SEM image. To assemble the SiO/PFM electrode with an active material loading as high as ~3 mg/cm^2,[8] 0.1 g PFM binder is dissolved in 2 g chlorobenzene. 0.9 g SiO particles are then added into the PFM binder solution and the slurry is homogenized for 1 hour before lamination. The doctor blade is set to a thickness of 150 µm to coat the electrode laminate.

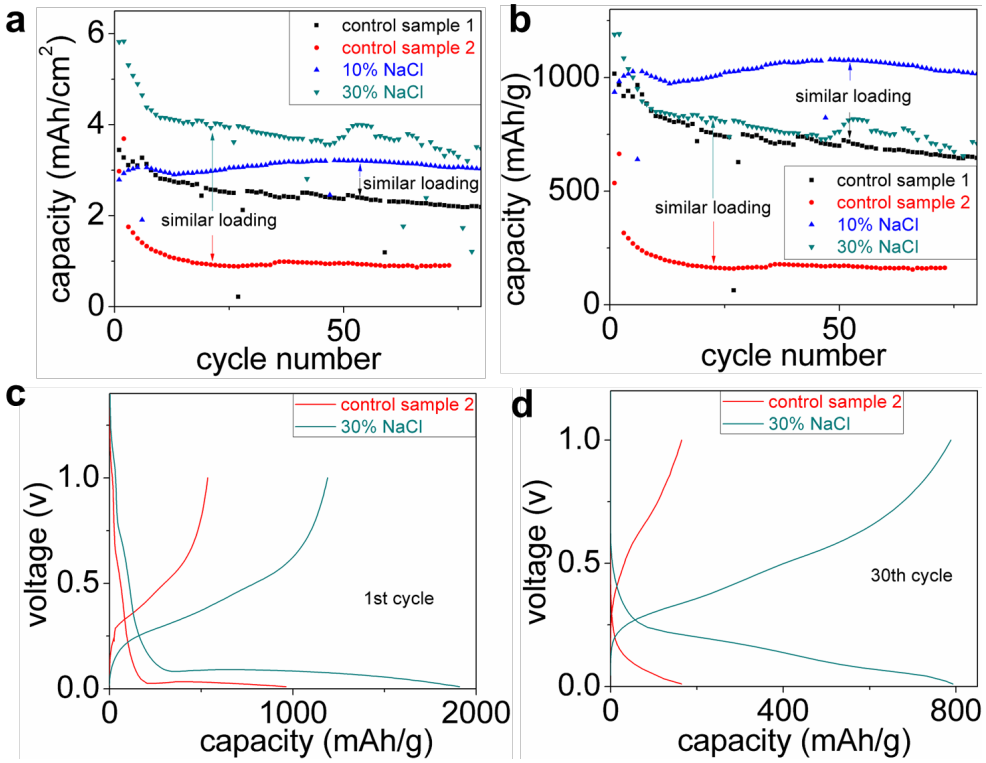

Figure 2. Cycling performance of the SiO/PFM electrodes with or without NaCl. (a) Areal capacity vs. cycle number, (b) Specific capacity vs. cycle number. (c) First and (d) thirtieth cycle voltage curves of samples with or without NaCl.

The maximum areal capacity of the SiO/PFM anode prepared as described is only around 2.5 mAh/cm^2. To increase the areal capacity, ball-milled NaCl is added during the slurry preparation process. The anode is allowed to dry under ambient conditions and is then washed with water for overnight before being vacuum-dried prior to coin cell assembly.

Control samples without NaCl and samples with modified electrode architecture (porosity generated by NaCl) were fabricated with similar material loadings in order to facilitate

comparison. Figure 2 shows the influence of adding NaCl on the electrochemical performance of SiO anode. Black (3.39 mg SiO/cm^2) and blue (3.00 mg SiO/cm^2) curves correspond to electrodes with similar loadings and show the influence of including 10 wt% ball-milled NaCl. Red (5.26 mg SiO/cm^2) and palegreen (4.89 mg SiO/cm^2) curves have similar SiO loadings and show the influence of 30 wt% NaCl.

The control sample (control smaple 1) with 3.39 mg SiO/cm^2 exhibits gradual capacity decay over cycling (black curve). For this relatively low loading, 10% NaCl is enough to generate sufficient internal porosity to stabilize the cycling performance, allowing an areal capacity of above 3 mAh/cm^2 to be maintained over 100 cycles at a C/10 rate (0.3 mA/cm^2). A control sample (control sample 2) with active material loading as high as 5.56 mg SiO/cm^2 almost shows cell failure after a couple of cycles at C/10 (red curve). A larger amount of NaCl (30 wt%) is added to generate more internal porosity to accommodate the volume expansion of the active material particles and facilitate lithium ion transport, allowing an areal capacity of above 4 mAh/cm^2 to be maintained over the 1st 30 cycles at a C/10 rate (0.49 mA/cm^2). Note that the relatively noisy data are common for the high-loading cells in this work, presumably due to the evolution of electrical contact during cell cycling. The voltage curves for the improvement of electrodes with a high material loading (control sample 2) are shown in Figure 2c and 2d. The effect of porosity generation is quite clear even for the 1st cycle, permitting access to almost theoretical lithiation (1900 mAh/g) and delithiation (1100 mAh/g) capacities of the SiO anode. A higher porosity should facilitate lithium ion transport and increase exposure of SiO active material particles to electrolyte solution. Both factors may contribute to the successful recovery of the full capacities of the active SiO materials.

Two important parameters are used to macroscopically describe the porous electrodes, electrode tortuosity (τ) and electrode porosity (ε). High tortuosity can hinder the rate of ion transport through the porous electrode network. Tortuosity and porosity are traditionally assumed to be related through the Bruggeman relation.[9]

$$\tau = \epsilon^{-\alpha} \tag{1}$$

This relation suggests that increased porosity is associated with decreased tortuosity. Both changes should facilitate lithium ion transport during cell operation, promoting the enhanced material loading and stabilized cycling performance seen in Figure 2.

		Control sample 1	10% NaCl	Control sample 2	30% NaCl
1st cycle	Q_c[a](mAh/g)	1016.4	935.2	535.6	1189.1
	η[b] (%)	62.14	63.08	55.61	62.30
10th cycle	Q_c[a] (mAh/g)	829.7	998.7	212.0	849.3
	η[b] (%)	96.77	98.87	98.35	98.99
70th cycle	Q_c[a] (mAh/g)	659.8	1035.9	163.1	711.67
	η[b] (%)	99.33	99.43	99.92	99.50

[a] charge (delithiation) capacity [b] coulombic efficiency

Table 1. Electrochemical parameters of the cell with or without porosities generated by NaCl.

The major electrochemical parameters of the cells profiled in Figure 2 are listed in Table 1, where again, it is only meaningful to compare electrodes with similar loadings. Incorporating 10 wt% NaCl probably does not generate enough porosity to significantly modify the initial cycling performance of the SiO electrode, as the capacity decay at this loading (~ 3 mg SiO/cm^2) only occurs after 10 cycles. Control sample 1 and the samples with 10% NaCl show only minor differences in performance initially, although the electrode with 10% NaCl shows higher coulombic efficiency (CE) and capacity retention over the rest of the cycling process. At an active material loading as high as ~ 5 mg SiO/cm^2, the sample with 30 wt% NaCl shows a large difference even at the first cycle. The charge capacity is improved to 1189 mAh/g from a value of

535.6 mAh/g in control sample 2, presumably due to the improved access of lithium ion to the active material particles. Although it starts with a high capacity, the modified electrode is able to retain ~60% of its initial capacity, compared to ~30% for the control sample.

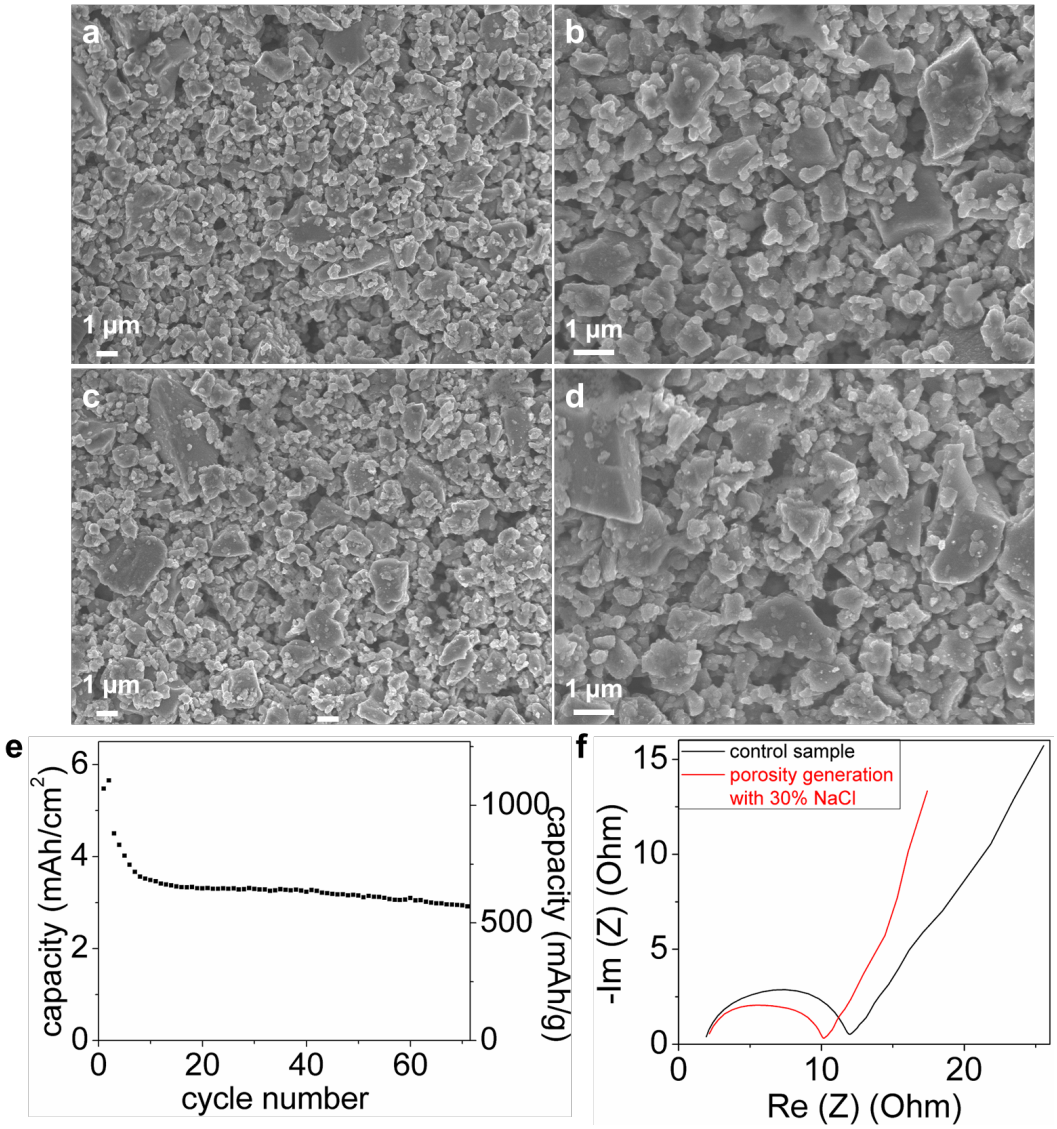

Figure 3. (a) (b) Top-view SEM images the control SiO electrode. (c) (d) Top-view SEM images of the SiO electrode with more porosities generated by NaCl. (e) Cycling performance of the SiO/PFM electrodes with porosity generation, C/10 for the first two cycles then C/3 (1.7 mA/cm2) (f) cell impedance of the SiO/PFM half cell with or without porosity generation using 30 wt% NaCl.

Many previous studies on high-loading Si anodes only demonstrate cell cycling at small charge/discharge rates (C/10 or even C/20), which is not ideal for practical applications; practical cycling experiments should be at a C/3 rate or higher. The rate capabilities of LIBs can be improved by structuring the porous electrodes appropriately, and we now discuss the effectiveness of our technique from this perspective.

From dimensional analysis, the characteristic time for lithium ion diffusion through an electrode material (τ_{eq}) is determined by the following relation

$$\tau_{eq} \sim L^2/D \quad (2)$$

where L is the diffusion length and D is the diffusion coefficient. To decrease the diffusion time and improve the rate capability of the cell, one can either decrease the diffusion length (by using electrode material particles with smaller dimensions) or increase the diffusion coefficient (by developing a better lithium ion conductor).[10] The former approach avoids changes in the battery chemistry and has a larger effect on the diffusion time due to the exponent of the diffusion length. The use of nano-material particles instead of micro-size particles can effectively decrease the diffusion length, although a good electrode architecture with optimized porous structure is critical to utilize this nano- or micro- active material particles.[3] To demonstrate the capability of our high-porosity Si-based anode towards this practical application, a high loading SiO/PFM anode with porosity generated by 30 wt% NaCl was cycled at C/10 for 2 cycles as a formation step, and C/3 long-term cycling was then performed. As shown in Figure 3a, an areal capacity of 3 mAh/cm^2 was still maintained at this high current density (1.7 mA/cm^2). As far as we know, this is one of the highest reported areal loadings for a Si-based anode at such a high charge/discharge rate, and we again note that the electrode as used was only composed of active material and polymer binder without any carbon conductive additives.

Impedance data from the half cells based on electrodes with or without NaCl is shown in Figure 3f. The sample cells initially went through a formation cycle at C/10, and impedance was measured at half lithiation, since cell potentials were relatively stable at that stage. The electron conduction of a half cell can be separated into two different ranges. Long-range conduction describes the process by which the electrons move from the current collector through the bulk electrode laminate, which is inversely proportional to the high frequency intercept of the impedance sweep. Typically, long-range conductivity corresponding to high frequency impedance is not a limiting parameter for the electrode impedance. However, short-range conduction corresponding to low frequency impedance is a limiting factor; it describes the process by which charge transfer at the electrode/electrolyte interface happens. With a higher internal porosity, the charge transfer impedance becomes smaller compared to that of the control electrodes.

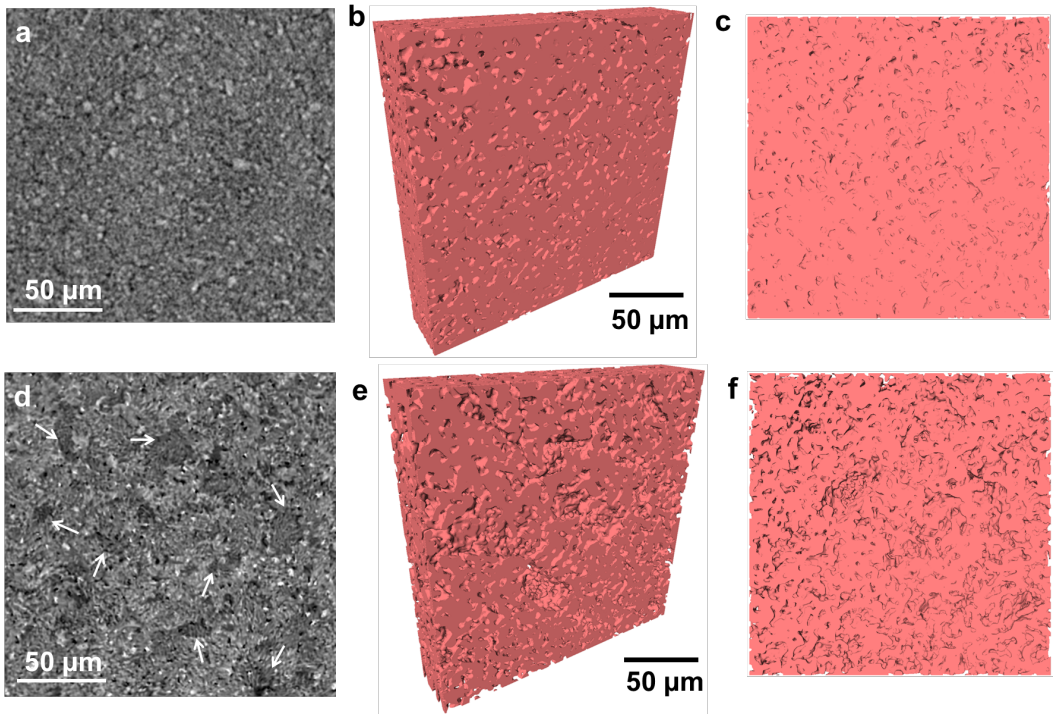

Figure 4. Tomographically reconstructed cross-section and volume rendering of (a) (b) (c) the control SiO/PFM electrode and (d) (e) (f) the SiO/PFM electrode with porosity generation. The pores induced by NaCl are marked with arros in the cross-section.

To further characterize the improved porous SiO electrode structure, we performed synchrotron X-ray microtomography on electrode samples at Beamline 8.3.2 of the Advanced Light Source (ALS). The pores formed from the normal slurry preparation/lamination process are visualized in the volume rendering shown in Figures 4b and 4c. These pores are important for electrolyte soaking and lithium ion transport, but at sizes of 1-10 µm, they are not able to accommodate the 50-100 % volume changes of the SiO particles during lithiation/delithiation. The extra pores generated by sacrificial NaCl particles, at sizes of 10-100 µm (Figure 4e and 4f), buffer the volume changes at the particle level, thereby enabling the improved electrochemical performance shown in Figure 2.

As a preliminary demonstration of the versatility of this method, improved electrochemical performance also was achieved with both nanoSi anodes and lithium iron phosphate cathodes. However, porosity generation by inclusion of NaCl is admittedly not a solution for all LIB electrode design limitations. This method only improves the areal capacity by 0.5~1.5 mAh/cm^2 beyond that obtained from electrodes fabricated in the usual way when the materials (active material, carbon additives and binder) and fabrication process otherwise remain the same. For example, while a stable areal capacity of 2.8 mAh/cm^2 was achieved with the original

SiO/conductive binder electrode, a final loading of 4 mAh/cm^2 was attained using the sacrificial NaCl method; similarly, in the nanoSi/conductive polymer electrode, the original loading was limited to ~1.5 mAh/cm^2 and was improved to 2.5 mAh/cm^2 through the introduction of NaCl.

Conclusions

A convenient and economical method was developed to control electrode porosity, enhancing the material loading and stabilizing the cycling performance of lithium ion electrodes. Sacrificial NaCl was added to a SiO electrode, which demonstrated an areal capacity of ~4 mAh/cm^2 at a C/10 rate (0.51 mA/cm^2) and an areal capacity of 3 mAh/cm^2 at a C/3 rate (1.7 mA/cm^2), one of the highest material loadings for a Si-based anode at such a high cycling rate. X-ray tomography confirmed the improved porous architecture of the SiO electrode using NaCl. Although a high-capacity lithium ion anode was used to illustrate the effect of this convenient pore generation method, the method described here should be applicable to many battery chemistries, including primary and secondary batteries using lithium ions, sodium ions, magnesium ions, aluminum ions or protons as the working.

References

1. Wu, H.; Cui, Y. *Nano Today* **2012,** *7*, 414-429.

2. Zhao, H.; Yuca, N.; Zheng, Z.; Fu, Y.; Battaglia, V. S.; Abdelbast, G.; Zaghib, K.; Liu, G. *ACS Appl. Mater. Interfaces* **2015,** *7*, 862-866.

3. Vu, A.; Qian, Y.; Stein, A. *Adv. Energy Mater.* **2012,** *2*, 1056-1085.

4. Liu, G.; Xun, S.; Vukmirovic, N.; Song, X.; Olalde-Velasco, P.; Zheng, H.; Battaglia, V. S.; Wang, L.; Yang, W. *Adv. Mater.* **2011,** *23*, 4679-4683.

5. Wu, M.; Xiao, X.; Vukmirovic, N.; Xun, S.; Das, P. K.; Song, X.; Olalde-Velasco, P.; Wang, D.; Weber, A. Z.; Wang, L. W.; Battaglia, V. S.; Yang, W.; Liu, G. *J. Am. Chem. Soc.* **2013,** *135*, 12048-56.

6. Dai, K.; Zhao, H.; Wang, Z.; Song, X.; Battaglia, V.; Liu, G. *J. Power Sources* **2014,** *263*, 276-279.

7. Zhao, H.; Wang, Z.; Lu, P.; Jiang, M.; Shi, F.; Song, X.; Zheng, Z.; Zhou, X.; Fu, Y.; Abdelbast, G.; Xiao, X.; Liu, Z.; Battaglia, V. S.; Zaghib, K.; Liu, G. *Nano Lett.* **2014,** *14* 6704-6710.

8. Song, J.; Zhou, M.; Yi, R.; Xu, T.; Gordin, M. L.; Tang, D.; Yu, Z.; Regula, M.; Wang, D.

Adv. Funct. Mater. **2014,** *24*, 5904-5910.

9. Bruggeman, D. A. G. *Annalen der Physik* **1935,** *416*, 636-664.

10. Etacheri, V.; Haik, O.; Goffer, Y.; Roberts, G. A.; Stefan, I. C.; Fasching, R.; Aurbach, D. *Langmuir* **2011,** *28*, 965-976.

ASSOCIATED CONTENT

Supplementary Information

Details about battery assembly and testing, and X-ray tomography. The Supporting Information is available free of charge on the ACS Publications website at DOI:

AUTHOR INFORMATION

Corresponding Author

*E-mail: gliu@lbl.gov

Notes

The authors declare no competing financial interests.

ACKNOWLEDGEMENTS

This work was funded by the Assistant Secretary for Energy Efficiency, Vehicle Technologies Office of the U.S. Department of Energy (U.S. DOE) under the Advanced Battery Materials Research (BMR) and Applied Battery Research (ABR) Programs. X-ray tomography measurements and analysis were performed at Beamline 8.3.2 of the Advanced Light Source (ALS). Nuclear magnetic resonance spectroscopy (NMR) was performed at the Molecular Foundry. TEM was performed at the National Center for Electron Microscopy. All of these projects and facilities are supported by the Director, Office of Science, Office of Basic Energy Sciences, of the U.S. Department of Energy, under Contract # DE-AC02-05 CH11231. Neslihan Yuca expresses thanks for the funding provided by The Scientific and Technological Research Council of Turkey (TUBITAK) in Ankara, Turkey.

TOC